A Study on the Synchronous Response of General Rotor-Bearing Systems due to Initial Deformation

Seong-Wook Hong*
School of Mechanical Engineering, Kumoh National University of Technology, Kyungbuk 730-701, Korea
Yong-Gyu Seo
Top Engineering Co., Ltd. Kyungbuk 730-810, Korea
Jong-Heuck Park
KAERI, Taejon PO Box 105, Korea

Rotating machinery often encounters excessive vibration due to various excitation sources. Among others, the synchronous excitation due to rotating unbalance and initial deformation is acknowledged to be one of the major sources of vibration in rotor-bearing systems. In this paper, a synchronous response analysis method in the presence of the initial deformation is proposed to investigate the peculiar effect of the initial deformation on the response of general flexible rotor-bearing systems with rotational speed dependency and the anisotropy. Experiments are performed and compared with computational results to verify the proposed analysis method. Two numerical examples are also provided to illustrate the characteristics of the synchronous response of general rotor-bearing systems due to the initial deformation.

Key Words: Rotor-Bearing System, Synchronous Response, Initial Deformation, Unbalance, Anisotropy

1. Introduction

The synchronous response in rotor-bearing systems is measured and analyzed because of its importance in diagnosis, balancing and parameter identification of rotors [Ehrich 1992; Darlow 1987; Lee and Hong 1988]. It is well known that mass unbalance is the major source of the synchronous vibration in rotor-bearing systems. However, the presence of the initial deformation in a shaft also causes a synchronous vibration different from that with only mass unbalance, and consequently gives rise to confusion in the measurement and analysis of the synchronous responses in rotor-bearing systems. Unless the effect of the initial deformation on the synchronous vibration is taken into account, the presence of the initial deformation inevitably degrades the effectiveness of balancing in flexible rotor-bearing systems.

The effect of the initial deformation on the synchronous vibration has been discussed in several studies for simple, ideal rotors. Nicholas et al. studied the synchronous response and balancing method for an ideally bowed Jeffcott rotor [Nicholas et al 1976a, 1976b]. Flack et al. analyzed the response of a simple rotor with initial deformation and runout [Flack et al 1982]. Shiau and Lee examined the effect of the initial deformation for a simple rotor with disk skew and mass unbalance [Shiau and Lee 1989]. Kim et al [Kim et al. 1999] presented experimental results for a Jeffcott rotor with initial deforma-

* Corresponding Author,
E-mail : swhong@kumoh.ac.kr
TEL : +82-54-467-4214; **FAX** : +82-54-467-4231
School of Mechanical Engineering, Kumoh National University of Technology, 188 Shinpyung-dong, Kumi-si, Kyungbuk 730-701, Korea. (Manuscript **Received** October 16, 2000; **Revised** June 12, 2001)

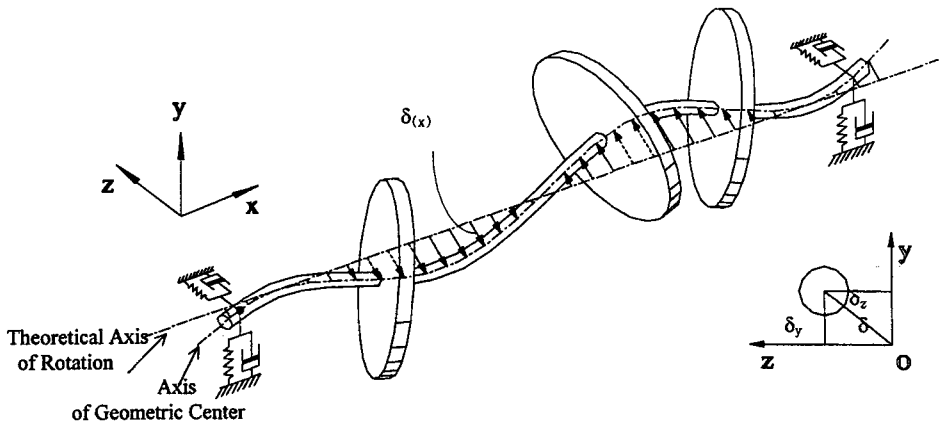

Fig. 1 A general rotor-bearing system with initial deformation

tion. The aforementioned papers have elucidated fundamental characteristics of the synchronous response caused by the initial deformation in ideal rotors. However, they have seldom dealt with general rotor-bearing systems that could be more realistic representations of rotor-bearing systems employed in practice.

The present study proposes a method for analyzing the synchronous vibration problem in the presence of both the initial deformation and mass unbalance. Investigations are made on the physics of general rotor-bearing systems with the initial deformation and mass unbalance. The anisotropy and rotational speed dependency due to bearings and gyroscopic effects are rigorously included in the system model. Experiments are made not only to observe the effect of the initial deformation but also to verify the proposed model and analysis method. Two illustrative examples are also presented to elucidate the characteristics of the synchronous response due to the initial deformation in general rotor-bearing systems.

2. Equations of Motion

A certain amount of permanent deformation in the shaft inevitably occurs during manufacturing and/or assembling processes for rotating machinery. In addition, there may exist a temporal deformation in the shaft due to unequal temperature distribution, axial load, material anisotropy, shaft rubbing, etc. The initial deformation of a rotor can be defined as a deviation of the axis of geometrical center from the theoretical axis of rotation as illustrated in Fig. 1. Then, the deviation of the shaft displacement from the initial deformation causes a restoring force for the shaft to be in line with the initial deformation. In the stationary condition, the shaft displacement (q) equals the initial deformation of the shaft (Δ). Thus, the finite element equation of the elastic rotor-bearing system subjected to the initial deformation can be written as

$$M^r\ddot{q}+\{C^c(\Omega)+\Omega G^r\}\dot{q} +\{K^r+K^c(\Omega)\}\{q-\Delta\}=f \tag{1}$$

or

$$M^r\ddot{q}+\{C^c(\Omega)+\Omega G^r\}\dot{q}+\{K^r+K^c(\Omega)\}q =f+\{K^r+K^c(\Omega)\}\Delta \tag{2}$$

where the superscripts r and c denote global matrices for rotor and connecting/supporting elements (couplings or bearings), respectively. The stiffness and damping matrices, $K^c(\Omega)$ and $C^c(\Omega)$, are generally nonsymmetric and rotational-speed-dependent, due to bearing characteristics. The inertia matrix M^r, and the stiffness matrix K^r are symmetric, while the gyroscopic matrix G^r is skew-symmetric. The order of all the matrices is $4n\times 4n$, n being the number of nodes for the finite element model. The matrices can be represented, using partitioned matrices, by

$$M^r=\begin{bmatrix}M & 0\\ 0 & M\end{bmatrix}\ G^r=\begin{bmatrix}0 & G\\ -G & 0\end{bmatrix}\ K^r=\begin{bmatrix}K & 0\\ 0 & K\end{bmatrix}$$
$$C^c=\begin{bmatrix}C_{yy} & C_{yz}\\ C_{zy} & C_{zz}\end{bmatrix}\ K^c=\begin{bmatrix}K_{yy} & K_{yz}\\ K_{zy} & K_{zz}\end{bmatrix} \tag{3}$$

where M, G and K are symmetric submatrices. The finite element coordinate vector q and the force vector f are

$$q=\begin{pmatrix}y\\ z\end{pmatrix}\ f=\begin{pmatrix}f_y\\ f_z\end{pmatrix} \tag{4}$$

where y and z are coordinate vectors in the y and z directions, respectively, and f_y and f_z the corresponding force vectors. As can be seen from Eq. (2), the initial deformation does not change the system matrices but engenders an external force dependent upon the system stiffness matrix. If the external force is due only to the mass unbalance, the force vector can be represented by

$$f=\begin{pmatrix}W\\ -jW\end{pmatrix}\Omega^2 e^{j\Omega t} \tag{5}$$

where

$$W=\{W_1\ 0\ W_2\ 0\cdots W_n\ 0\}^t$$

Here W is the complex mass unbalance vector, and W_i, $i=1, 2, \cdots, n$, is the complex unbalance at i-th node. On the other hand, the initial deformation vector, denoted by Δ, is represented as

$$\Delta=\begin{pmatrix}\delta_y\\ \delta_z\end{pmatrix}=\begin{pmatrix}\delta\\ -j\delta\end{pmatrix}e^{j\Omega t} \tag{6}$$

where

$$\delta=\{\delta_1\ \delta_{\theta_1}\ \delta_2\ \delta_{\theta_2}\cdots\delta_n\ \delta_{\theta n}\}^t$$

Here δ is the complex initial deformation vector in the rotor-attached frame, which contains the deviation of geometrical center from the theoretical axis of rotation at each node. The $\delta_i, \delta_{\theta i}$, $i=1,2, \cdots, n$ are the lateral and angular deformations of the shaft at i-th node, respectively.

While distributed mass unbalance can be lumped as discrete lateral excitation forces at nodes, the initial deformation has to be lumped with both the lateral and angular components at every node because the excitation due to the initial deformation is represented by the multiplication of the initial deformation and the stiffness matrix that includes elements associated with angular displacements. The excitation force due to the initial deformation may be thought of as an equivalent, distributed force needed to make the initially deformed shaft to be straight from the static point of view. Unless the angular deformation is taken into account, the force vector due to the initial deformation cannot constitute an equivalent force for satisfying the aforementioned condition. In fact, the angular deformation turns out to play an important role in determining the excitation force vector. On the other hand, the mass unbalance excitation is proportional to the square of the rotational speed, but the excitation due to the initial deformation is independent of the rotational speed. However, the excitation force due to the initial deformation could be implicitly dependent on the rotational speed if the stiffness matrix has the rotational speed dependency as can be expected from Eq. (2).

3. Synchronous Response Analysis Method

The direct inversion method is preferable in the synchronous response analysis of general rotor-bearing systems [Hong and Park 1997]. Introducing the complex displacement and force vectors defined as

$$p=y+jz,\ f=f_y+jf_z \tag{7}$$

Eq. (2) can be rewritten as

$$M\ddot{p}-j\Omega G\dot{p}+C_f\dot{p}+C_b\dot{\bar{p}}+Kp+K_f\bar{p}+K_b\bar{p}=f \tag{8}$$

where the subscripts f and b denote forward and backward, respectively, and '-' represents the complex conjugate. Here the complex damping and stiffness matrices for the connecting/supporting elements can be represented as

$$2C_f=C_{yy}+C_{zz}-j(C_{yz}-C_{zy}),\ 2C_b=C_{yy}-C_{zz}+j(C_{yz}+C_{zy})$$
$$2K_f=K_{yy}+K_{zz}-j(K_{yz}-K_{zy}),\ 2K_b=K_{yy}-K_{zz}+j(K_{yz}+K_{zy}) \tag{9}$$

The excitation vector in Eq. (8) can be represented as

$$f=\{W\Omega^2+(K+K_f)\delta\}e^{j\Omega t}+K_b\bar{\delta}e^{-j\Omega t} \tag{10}$$

Table 1 Specifications of the finite element model for the test rotor

Element		Property	Data
Shaft (24 elements)		Total length, m	1.2
		Diameter, cm	2.5
		Young's Modulus, GN/m^2	210
		Density, Kg/m^3	7726
Disk (3 identical)		Mass, Kg	3.575
		Polar moment of inertia, $Kg\text{-}m^2$	0.0176
		Diametral moment of inertia, $Kg\text{-}m^2$	0.00897
		Locations, m (from left)	0.4, 0.65, 1.19
Bearings	1	Kyy(=Kzz), MN/m	35
		Kyz(=Kzy), MN/m	0
		Cyy(=Czz), Ns/m	0
		Cyz(=Czy), Ns/m	0
		Location, m (from left)	0.104
	2	Kyy(=Kzz), MNm	6
		Kyz(=Kzy), MN/m	0
		Cyy(=Czz), Ns/m	300
		Cyz(=Czy), Ns/m	0
		Location, m (from left)	0.896

In general, the synchronous response is composed of two components, forward and backward: i. e.,

$$p=p_f e^{j\Omega t}+\bar{p}_b e^{-j\Omega t} \tag{11}$$

where p_f and p_b are the forward and backward whirl response vectors, respectively. Substitution of Eqs. (10) and (11) into Eq. (8) yields

$$\begin{pmatrix} p_f \\ p_b \end{pmatrix}=\begin{bmatrix} H_{ff} & H_{fb} \\ H_{bf} & H_{bb} \end{bmatrix}\begin{pmatrix} W\Omega^2+(K+K_f)\delta \\ \overline{K}_b\delta \end{pmatrix} \tag{12}$$

where

$$\begin{bmatrix} H_{ff} & H_{fb} \\ H_{bf} & H_{bb} \end{bmatrix}=\begin{bmatrix} D_{ff} & D_{fb} \\ D_{bf} & D_{bb} \end{bmatrix}^{-1}$$

and

$$\begin{aligned} D_{ff}&=-\Omega^2M+\Omega^2G+K+K_f+j\Omega C_f \\ D_{bb}&=-\Omega^2M-\Omega^2G+K+\overline{K}_f+j\Omega\overline{C}_f \\ D_{fb}&=K_b+j\Omega C_b,\ D_{bf}=\overline{K}_b+j\Omega\overline{C}_b \end{aligned} \tag{13}$$

Here H_{ff}, H_{bf}, H_{fb} and H_{bb} in Eq. (12) are the unbalance response functions that can be utilized to calculate unbalance responses or influence coefficients [Hong and Park 1997]. It is noteworthy that the excitation due to the initial deformation has both the forward and backward components as described in Eq. (12). In other words, the synchronous response due to the initial deformation for an anisotropic rotor system reflects all four unbalance response functions while the unbalance response is related only to H_{ff} and H_{bf}. The backward excitation caused by the initial deformation is dependent on the amount of the initial deformation and the stiffness of the bearing. For an isotropic rotor, Eq. (12) is reduced to

$$p_f=H_{ff}W\Omega^2+H_{ff}(K+K_f)\delta,\ p_b=0 \tag{14}$$

In this case, no backward whirl occurs because the initial deformation does not excite the backward whirl in isotropic systems. If there is no initial deformation at bearing positions, Eq. (12) should be rewritten as

$$p_f=H_{ff}W\Omega^2+H_{ff}K\delta,\ p_b=H_{bf}W\Omega^2+H_{bf}K\delta \tag{15}$$

In this case, the synchronous responses are governed only by H_{ff} and H_{bf}.

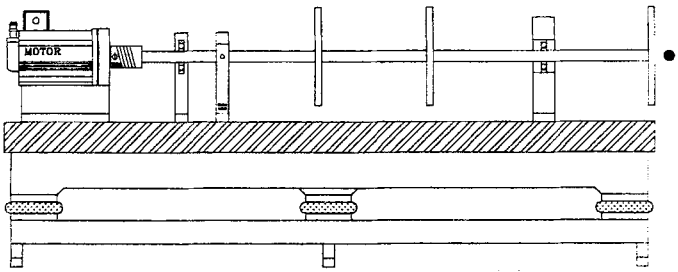

Fig. 2 Experimental test rig

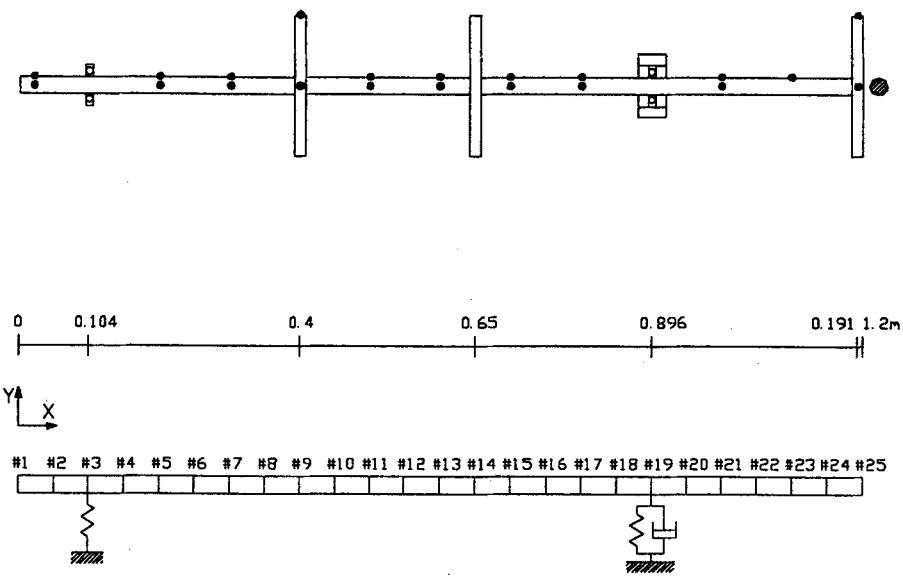

Fig. 3 The finite element model for the test rotor and the measurement points

4. Experimental Validation of the Analysis Method

4.1 Experimental set-up

Experiments are conducted to verify the proposed analysis method. Figure 2 shows the test rotor system, which is set on an air mounted steel bed, and composed of a shaft with the length of 1. 2m and the diameter of 0.025m, 3 identical disks, two ball bearings, and a leaf spring type vibration damper [Jei et al 1999] to prevent excessive vibration. Figure 3 shows the finite element model of the test rotor and also indicates the measurement points. Table 1 shows the specifications of the finite element model for simulating the experimental system. One bearing is installed at node 3 and the other, integrated with the vibration damper, is installed at node 19. Two gap sensors placed horizontally and vertically, respectively, are used for measuring the vibration response. The number of data points per revolution is kept at 256, independent of the rotational speed, by changing the sampling rate. A proximity sensor is placed right next to the coupling for triggering the data acquisition so as to start sampling at the same rotational angle.

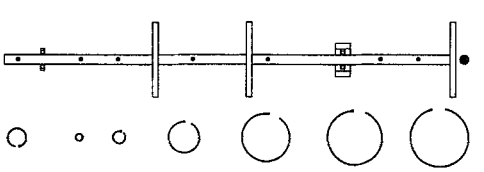

Fig. 4 Orbital plot at 100 rpm

Table 2 Comparison of theoretical and experimental natural frequencies for the test rotor

	1^{st} mode (Hz)		2^{nd} mode (Hz)		3^{rd} mode (Hz)	
	Ver.	Hor.	Ver.	Hor.	Ver.	Hor.
FEM	24.3	24.3	53.1	53.1	151.7	151.7
Experiment	24.3	24.3	55.5	55.5	160.7	158.7

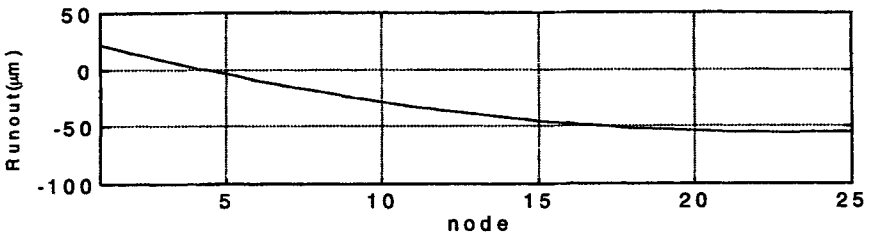

Fig. 5 The identified initial deformation of the test rotor

In general, it is possible to estimate the initial deformation of a rotor by measuring the synchronous response along the shaft when the rotor is rotating slowly. Two gap sensors are used to measure the initial deformation of the test rotor. Since the shape of the initial deformation is expected to be simple, interpolation of measured data at several selected positions may be good enough to obtain the initial deformation for positions other than the selected positions.

4.2 Preliminary test

The synchronous component is extracted by taking 1X component out of the Fourier transform of the sampled data. The initial deformation, which is almost in-plane as illustrated in Fig. 4, is obtained by measuring the synchronous response at 100 rpm.

Figure 5 shows the identified in-plane initial deformation. It is interesting to note that the magnitude of the initial deformation at the vibration damper is somewhat large and that the phase is not changed around the damper. A preliminary modal testing is made to check the adequacy of the finite element model. The first three natural frequencies obtained from the finite element model and experiments are compared in Table 2. The table shows that the finite element model can well represent the experimental system and that the system can be assumed to be isotropic, at least,

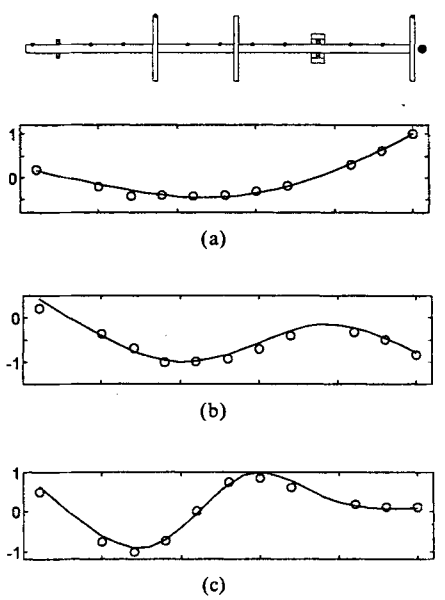

Fig. 6 Comparison of theoretical and experimental mode shapes

in the operating speed range of interest (0~2000 rpm). Figure 6 compares computed and experimental mode shapes. This result again assures the adequacy of the finite element model.

4.3 Experiment and simulation

Figure 7 shows the synchronous responses of the test rotor measured along the shaft. Since insignificant backward responses are observed, only forward components are shown here. The

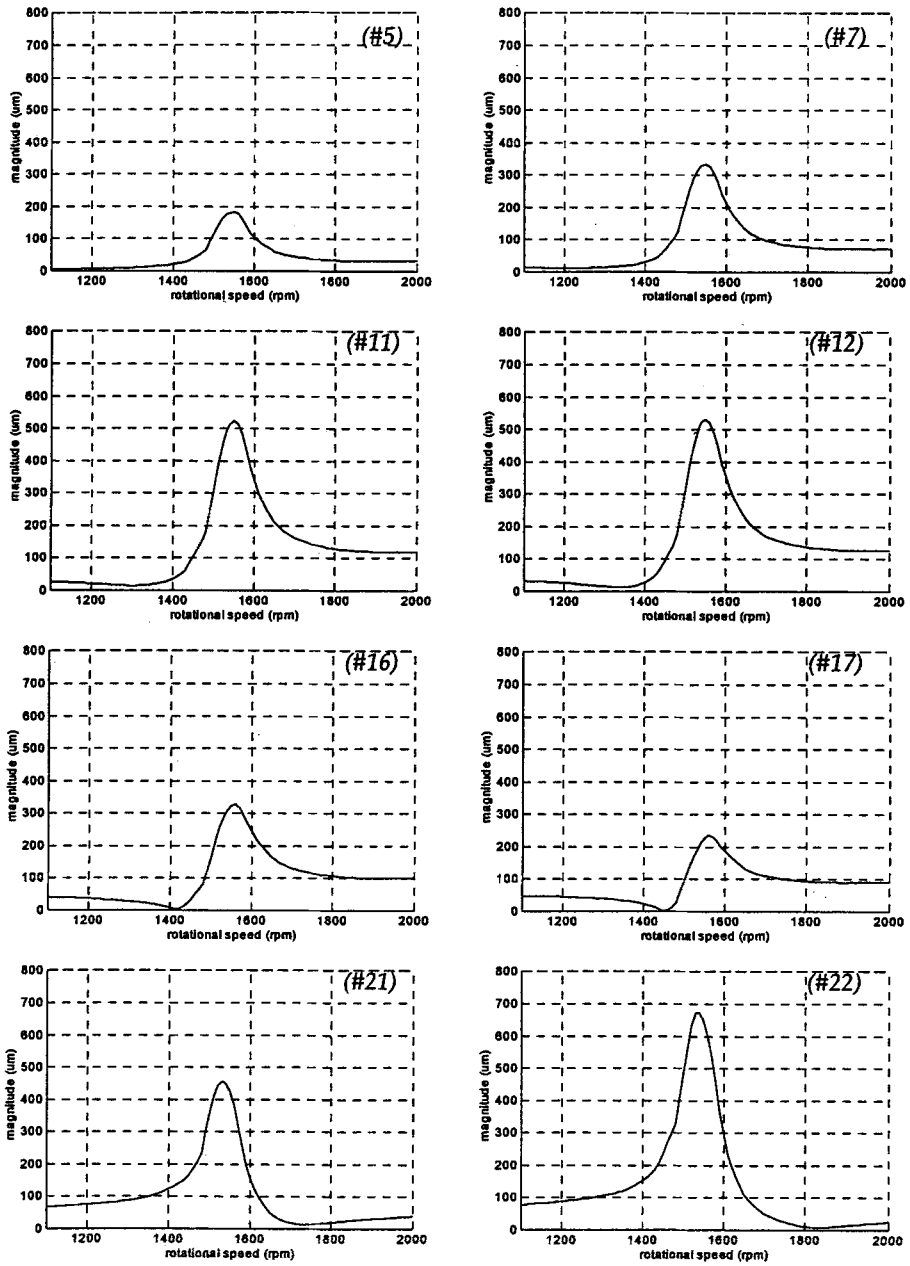

Fig. 7 Experimental synchronous response of test rotor-bearing system

measured synchronous responses due to the initial deformation reveal a rather peculiar characteristic in that the amplitude of the synchronous response becomes zero at a certain rotational speed. This characteristic, which is obviously different from the unbalance response, is closely related with the shape of the initial deformation. Figure 8 shows the simulation results for the responses due to the initial deformation. The simulation also shows that the synchronous response due to the measured initial deformation can be zero at a certain rotational speed. Although the simulated responses given in Fig. 8 are qualitatively in good agreement with the measured responses reported

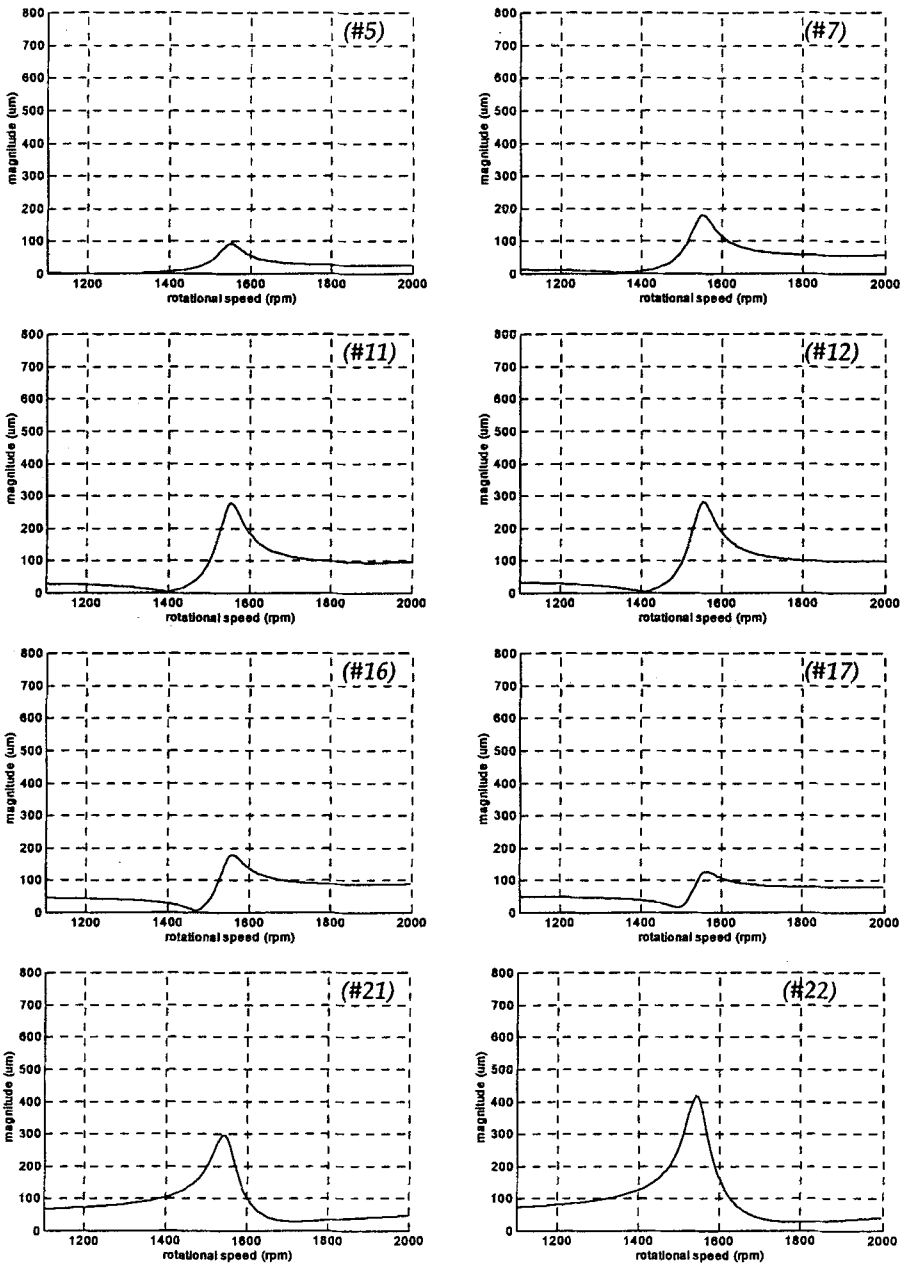

Fig. 8 Simulated synchronous response due to the initial deformation

in Fig. 7, the magnitudes of the simulated responses are less than those of the measured responses. The reason is that the measured synchronous response is also affected by the residual unbalance in the rotor system. To simulate a more realistic situation, the synchronous responses due to the mass unbalance as well as the initial deformation are computed. Since the unbalance distribution is not known *a priori*, the amount and phase of the unbalances are adjusted

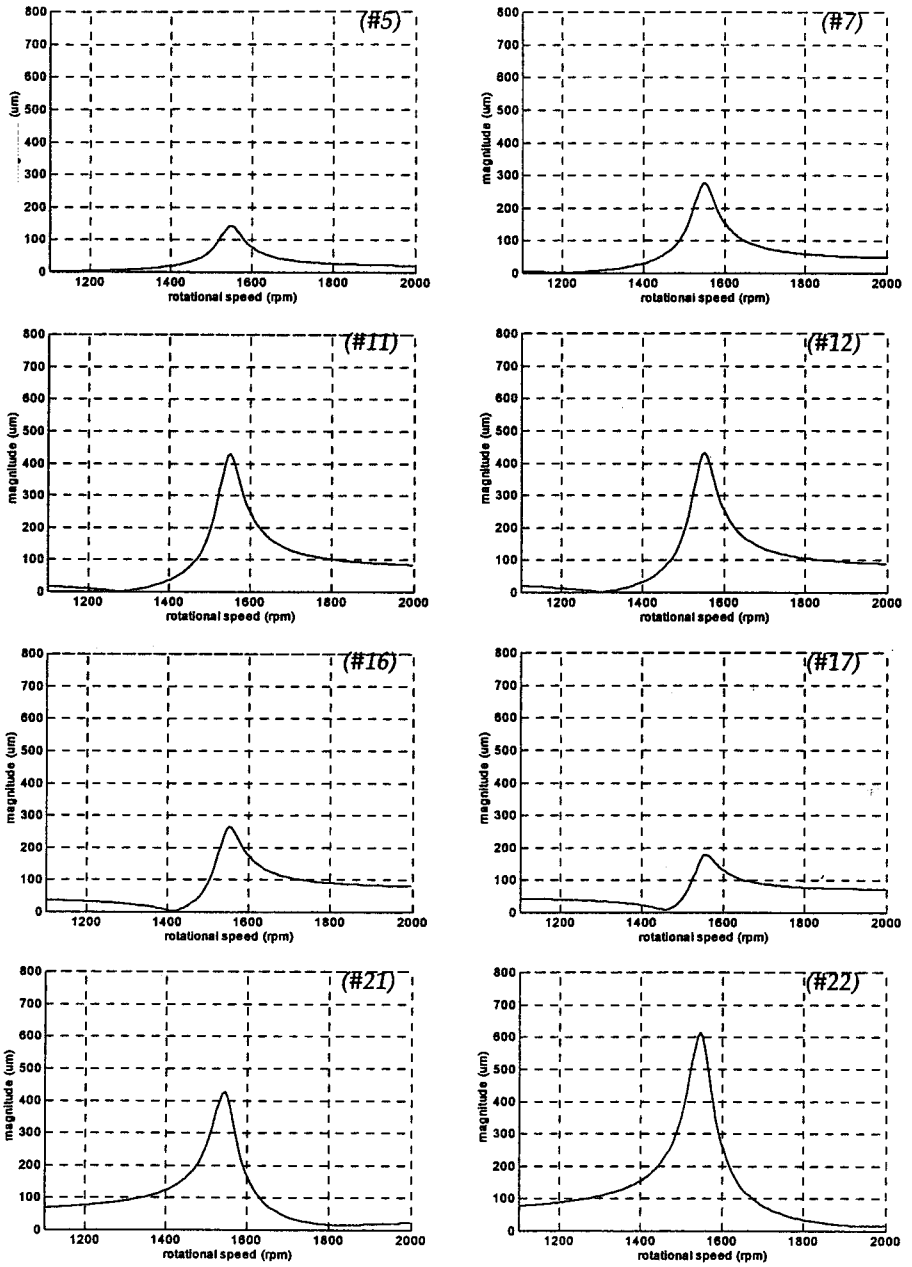

Fig. 9 Simulated synchronous response in the presence of initial deformation and unbalance

to match the computed responses with the measured responses under the assumption that discrete unbalances are present only at the disks. Figure 9 shows the simulated responses due to both the initial deformation and the residual unbalance. The simulated responses agree well with the experimental responses both qualitatively and quantitatively. This result assures that the proposed model can predict the experimental results quite well.

5. Numerical Study

Numerical experiments are performed to inves-

Table 3 Specifications of the numerical model

Element		Property	Data
Shaft		Length, m	1.2
		Diameter, cm	8.0
		Young's Modulus, GN/m^2	200
		Density, Kg/m^3	8000
Disk (3 identical)		Mass, Kg	20
		Polar moment of inertia, $Kg-m^2$	0.163
		Diametral moment of inertia, $Kg-m^2$	0.085
		Locations, m (from left)	0.4, 0.5, 1.2
Bearings	1	Load, Kgf	29.42
		Location, m (from left)	0
		L/D, C/R	0.5, 2/1000
		Viscosity, mPa. s	9.37
	2	Load, Kgf	78.84
		Location, m (from left)	0.9
		L/D, C/R	0. 5, 2/1000
		Viscosity, mPa. s	9.37

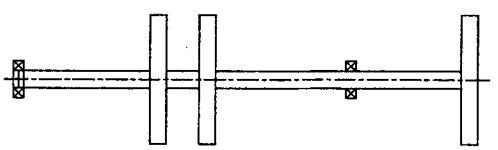

Fig. 10 Numerical model

tigate the vibration characteristics of a general rotor-bearing system with initial deformations. In order to rigorously investigate the characteristics of rotor-bearing systems with rotational speed dependency and the anisotropy, a rotor-bearing system with fluid film type bearings is exemplified. The current rotor-bearing system model, which is shown in Fig. 10, is taken from the numerical model reported in a reference [Hong and Park 1997]. Figure 11 shows the assumed initial deformation, which is represented as a third order polynomial function of the shaft axial position. Table 3 shows the specifications of the rotor system considered. The finite element model consists of 12 identical shaft elements, 3 identical rigid disks, and 2 fluid film type bearings. The bearing characteristics are approximated as second order polynomial functions of rotational speed over the data provided in [Someya 1988]. Two types of fluid film bearing-isotropic 4 pad tilting pad bearing and anisotropic 5 pad tilting pad bearing-are considered.

5.1 Example 1: Rotor with isotropic bearings

The rotor system is assumed to have two LBP type 4 pad tilting-pad bearings with the preload angle of 80° and the preload factor of 0. In this case, the system is isotropic. The difference between the two bearings is the loads applied to the bearings. The problem here is to compare the responses caused by the mass unbalance and the initial deformation. Figure 12 shows the synchronous responses by the initial deformation only, by the mass unbalance only, and by both, respectively. The unbalance is assumed to be 200 g-mm and in phase with the initial in-plane deformation. Orbital plots due to the initial deformation at some selected rotational speeds are shown in Fig. 13. As expected, no backward response is observed. In particular, the response due to the initial deformation is quite different from that due to the mass unbalance in the low speed region. It is interesting to note that the initial deformation dominates the response in a

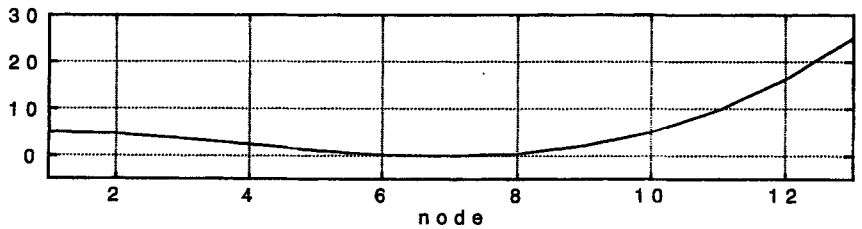

Fig. 11 Initial deformation used in the numerical experiment

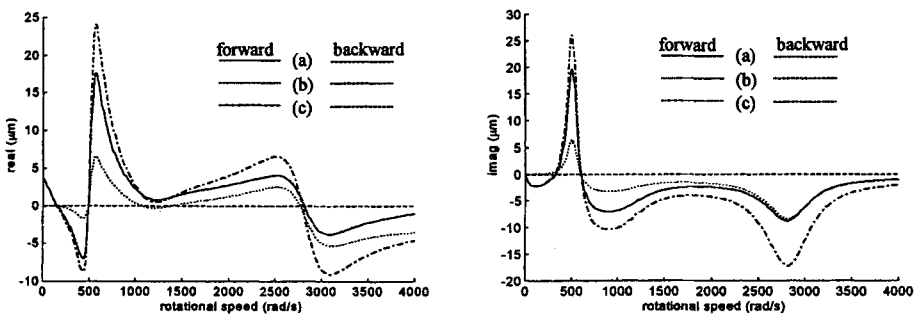

Fig. 12 Responses at node 3 for example 1 ; (a) Synchronous response due to the initial deformation (b) unbalance response with an unbalance at node 13 (c) Synchronous response in the presence of both initial deformation and unbalance

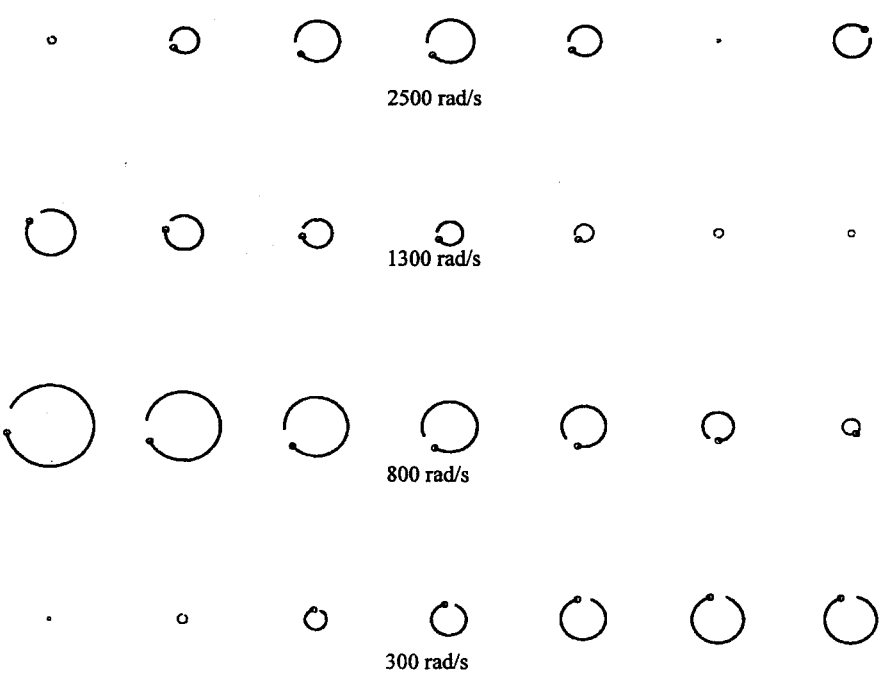

Fig. 13 Orbital plot due to initial deformation for example 1

lower speed region while the effect of mass unbalance becomes dominant in a higher speed region. It can be concluded that the effect of the initial deformation may be neglected in the higher speed region as long as it is not significantly large in the low speed region.

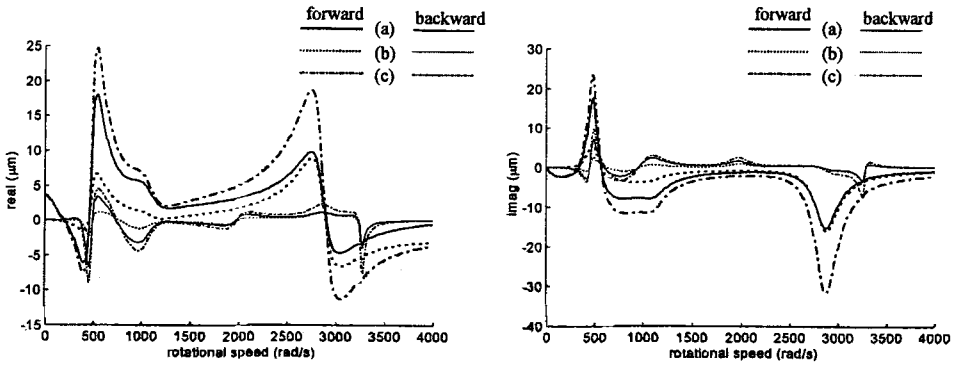

Fig. 14 Responses at node 3 for example 2; (a) Synchronous response due to the initial deformation (b) unbalance response with an unbalance at node 13 (c) Synchronous response in the presence of both initial deformation and unbalance

5.2 Example 2: Rotor with anisotropic bearings

This example presents a rotor system supported by two LBP type 5 pad tilting-pad bearings with the preload angle of 60° and the preload factor of 0. These two bearings are anisotropic by nature. The purpose of this example is to see the effect of the anisotropy on the synchronous vibration due to the initial deformation. The same unbalance as in example 1 is applied to the system. Figure 14 shows the synchronous responses by the initial deformation only, by the mass unbalance only, and by both, respectively. Figure 14 indicates that the initial deformation causes the backward excitation as well as the forward excitation. In other words, the responses due to the initial deformation reflect all the unbalance response functions. As in the previous example, the effect of the initial deformation dominates the responses in the low speed region. Orbital plots due to the initial deformation at some selected rotational speeds are shown in Fig. 15. Unlike the previous example, the orbits are elliptical due to the existence of both the forward and backward whirl components.

6. Concluding Remarks

This paper deals with an effective analysis method for obtaining the dynamic responses of general rotor-bearing systems in the presence of the initial deformation. The proposed analysis method is shown to be valid through a series of simulations and experiments. In addition, the physical characteristics of the synchronous response due to the initial deformation are discussed with experimental results and two numerical examples. For the analysis of rotors subjected to the initial deformation, both the lateral and angular deformations have to be considered in modeling because the excitation due to the initial deformation is represented by the multiplication of the initial deformation vector and the stiffness matrix of the rotor-bearing system. The initial deformation can provide a backward excitation to an anisotropic system. Through the experiments and simulations, it is found that the synchronous response can be zero at a certain speed, the value of which is dependent on the measurement position, shape of the initial deformation, and distribution of the mass unbalance. The initial deformation effect dominates the synchronous response in low speed regions while the mass unbalance effect becomes dominant in higher speed regions. However, the presence of both the mass unbalance and the initial deformation in a rotating shaft may cause confusion and/or measurement error during balancing and vibration diagnostics of rotor-bearing systems. Thus, it is believed that simulations based on the proposed method together with the measured initial deformation can be of use in identifying the characteristics of measured synchronous response, and thus in

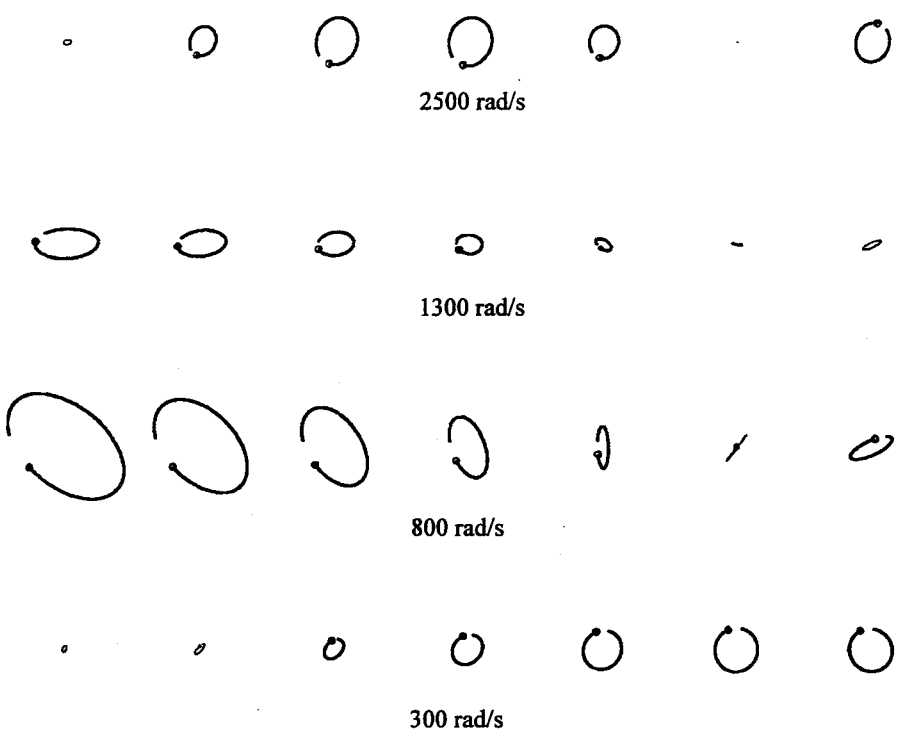

Fig. 15 Orbital plot due to initial deformation for example 2

enhancing the performance of balancing and vibration diagnostics.

References

Darlow, M. S., 1987, "Balancing of High Speed Machinery: Theory, Method, and Experimental Results," *Mechanical Systems and Signal Processing*, Vol. 1, No. 1, pp. 105~134.

Ehrich, F. F., 1992, *Handbook of Rotor Dynamics*, McGraw-Hill, New York.

Flack, R. D., et al., 1982, "Comparison of the Unbalance Responses of Jeffcott Rotors with Shaft Bow and Shaft Runouts," *ASME Journal of Mechanical Design*, Vol. 104, No. 2, pp. 318~328.

Hong, S. W. and Park, J. H., 1997, "An Efficient Method for the Unbalance Response Analysis of Rotor-Bearing Systems," *Journal of Sound and Vibration*, Vol. 200, No. 4, pp. 491~504.

Jei, Y. G., Kim, J. S., Jung, S. Y. and Hong, S. W., 1999, "A Lateral Vibration Damper Using Leaf Springs," *Trans. KSME A*, Vol. 22, No. 4, 843~858.

Kim, B. O., Kim, B. K. and Kim YC., 1999, "An Experimental Study on the Dynamic Characteristics of a Shaft with Initial Deflection," *Trans. KSAE*, Vol. 7, No. 3, 178~184.

Lee, C. W. and Hong, S. W., 1989, "Identification of Bearing Dynamic Coefficients by Unbalance Response Measurements," *Proceedings of the Institution of Mechanical Engineers, Journal of Mechanical Engineering Science*, Vol. 203C, pp. 93~101.

Nicholas, J. C., et al., 1976, "Effect of Residual Shaft Bow on Unbalance Response and Balancing of a Single Mass Flexible Rotor: Part I-Unbalance Response," *ASME Journal of Engineering for Power*, Vol. 98, No. 2, pp. 171~181.

Nicholas, J. C., et al., 1976, "Effect of Residual Shaft Bow on Unbalance Response and Balancing of a Single Mass Flexible Rotor: Part II-Balancing," *ASME Journal of Engineering for Power*, Vol. 98, No. 2, pp. 182~189.

Shiau, T. N. and Lee, E. K., 1989, "The Residual Shaft Bow Effect on Dynamic Response of the Simply Supported Rotor with Disk Skew and Mass Unbalances," *ASME Journal of Vibrations, Acoustics, Stress, and Reliability in Design*, Vol. 111, pp. 170~178.

Someya, T., 1988, *Journal Bearing Databook*, Spring-Verlag.